ORGANOMETALLICS

Article

pubs.acs.org/Organometallics

Pyridine-Stabilized Fast-Initiating Ruthenium Monothiolate Catalysts for *Z*-Selective Olefin Metathesis

Giovanni Occhipinti,* Karl W. Törnroos, and Vidar R. Jensen*

Department of Chemistry, University of Bergen, Allégaten 41, N-5007 Bergen, Norway

Supporting Information

ABSTRACT: Pyridine as a stabilizing donor ligand drastically improves the performance of ruthenium monothiolate catalysts for olefin metathesis in comparison with previous versions based on a stabilizing benzylidene ether ligand. The new pyridine-stabilized ruthenium alkylidenes undergo fast initiation and reach appreciable yields combined with moderate to high *Z* selectivity in self-metathesis of terminal olefins after only a few minutes at room temperature. Moreover, they can be used with a variety of substrates, including acids, and promote self-metathesis of ω-alkenoic acids. The pyridine-stabilized ruthenium monothiolate catalysts are also efficient at the high substrate dilutions of macrocylic ring-closing metathesis and resist temperatures above 100 °C during catalysis.

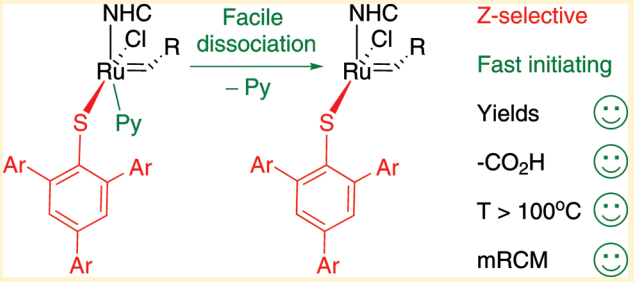

INTRODUCTION

Transition-metal-catalyzed olefin metathesis is a powerful, versatile, and green method for making carbon−carbon double bonds and is widely used in organic synthesis.[1,2] This reaction is also exploited in several industrial processes ranging from value-added processes of simple alkenes to the synthesis of complex pharmaceuticals.[3,4]

Grubbs-type ruthenium-based catalysts have been the most widely used so far because, in addition to their high activity, they tolerate many functional groups, including alcohols and carboxylic acids.[5] Moreover, they are relatively robust toward air and moisture and therefore also easy to handle and store. All this means that the ruthenium-based catalysts may be used in a broad range of synthetic applications.[6−21] Nevertheless, apart from particular cases, they do not give *Z*-configured alkenes in practical yields. Thus, to fill this need, highly *Z* selective olefin metathesis systems based on Mo,[22] W,[23] and Ru[24−26] have been developed in recent years (see Chart 1 for examples). These catalysts, with the exception of the stereoretentive Ru dithiolate complexes,[27,28] get their *Z* selectivity from a "wall" of steric bulk that essentially blocks one of the two faces of the metallacyclobutane moiety in the rate-determining transition state.[29−31] Overall, these compounds allow the selective synthesis of many useful cis-disubstituted alkenes in moderate to high yields.[32−35]However, none of the existing *Z*-selective systems can compete with the nonstereoselective Grubbs-type catalysts in terms of robustness, catalytic activity, and functional group tolerance, all of which still limit the scope of *Z* selective metathesis despite the impressive progress in recent years.

Z-Selective ruthenium-based catalysts have been achieved by following two conceptually different strategies (see Figure 1). The first strategy exploits the steric properties of the N-heterocyclic carbene (NHC) ligand in a side-pathway mechanism,[25,29] exemplified by the cyclometalated ruthenium catalysts (e.g., **3**, Chart 1) developed by Grubbs and co-workers[24,36,37] and by the Ru dithiolate systems (e.g., **4**, Chart 1) developed by Hoveyda and co-workers.[25,38] The Ru dithiolates are highly stereoretentive but are much more active

Chart 1. Examples of *Z*-Selective Catalysts

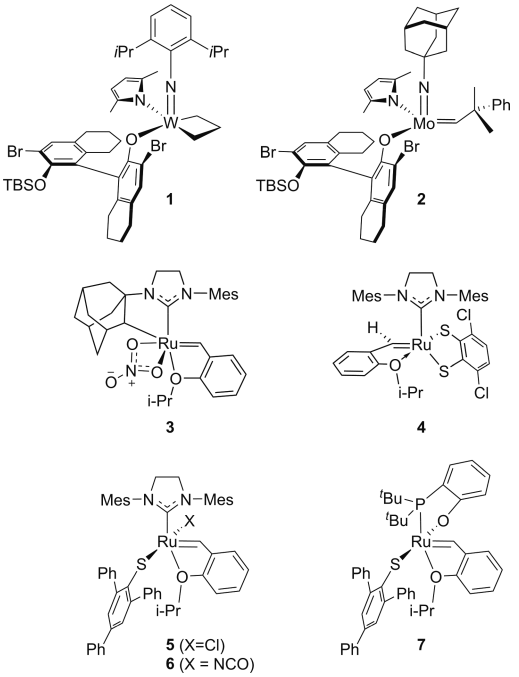

Received: June 12, 2017
Published: August 21, 2017

DOI: 10.1021/acs.organomet.7b00441
Organometallics 2017, 36, 3284−3292

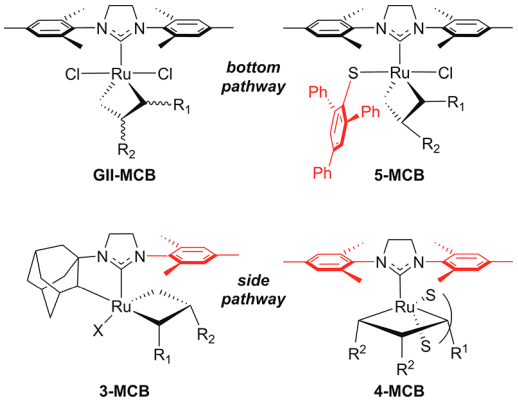

Figure 1. Geometry of the metallacyclobutane intermediate resulting from bottom (**GII** and **5**) and side (**3** and **4**) olefin binding pathways. For the *Z*-selective catalysts **3**–**5** the substituents R^1 and R^2 of the metallacyclobutane ring prefer to be oriented away from the sterically demanding moieties, rendered in red. For the *Z*-selective catalysts, the favored cis configuration of the metallacyclobutane is shown.

and efficient in *Z*-selective in comparison to *E*-selective reactions.[27] Grubbs and co-workers have recently improved the original design to boost the catalytic performance of the *E*-selective transformations.[28] The second strategy to achieve *Z*-selective Ru-based catalysts consists of retaining the bottom-pathway mechanism of the parent Grubbs-type catalysts[39−42] at the same time as using anionic ligands of very different size.[26,43−48]

The only family of *Z*-selective catalysts following a bottom-pathway mechanism are ruthenium monothiolate alkylidenes such as complexes **5**–**7** (Chart 1), which are moderately to highly selective and reach 96% *Z* selectivity in the self-metathesis of sterically hindered allylic substrates such as allyltrimethylsilane.[26,46−48] These compounds share most of the structural features and the bottom-pathway mechanism[30] with the Hoveyda−Grubbs-type catalysts (see the upper part of Figure 1) and have been developed, via computational prediction and experimental followup, by our group.[46−48] The catalysts are prepared from commercially available or easily accessible nonselective Hoveyda−Grubbs-type catalysts via one-step replacement of one of the anionic ligands (e.g., chloride or isocyanate) by a sterically demanding thiolate (e.g., 2,4,6-triphenylbenzenethiolate).

Whereas the monothiolate-substituted catalysts so far have been both less *Z*-selective and less active than side-pathway catalysts, they may inherit highly desirable properties such as robustness from the parent catalyst.[49] For example, compound **6** (Chart 1) can be used in air with nondegassed and nonpurified substrates and solvents and tolerates the presence of acidic additives.[47] To benefit from this robustness and functional group tolerance in practical metathesis experiments, however, the *Z*-product yields from the monothiolate-substituted catalysts must be increased. The yields have so far been hampered by low catalytic activity combined with a high tendency to isomerize both substrates and products. With the monothiolate-substituted catalysts, appreciable metathesis activity is typically only obtained at high substrate concentrations and at moderately elevated temperatures, while isomerization reactions reduce the metathesis efficiency at elevated temperatures and at high substrate dilution. For instance, the catalytic performance at the high substrate dilutions of macrocyclic ring-closing metathesis (mRCM) is poor.[50,51]

In this contribution we overcome the main limitations of the monothiolate-substituted catalysts by replacing the chelating *o*-isopropoxybenzylidene ligand with monodentate alkylidenes and pyridine. The new catalysts initiate metathesis more quickly and are also much less prone to mediate olefin isomerization. The improved metathesis performance of the new catalysts is particularly evident from the fact that they allow *Z*-selective synthesis of α,ω-dicarboxylic acid alkenes via self-metathesis of ω-alkenoic acids, an application that facilitates access to many biologically active targets but that has not yet been achieved with other *Z*-selective catalysts.[52,53]

RESULTS AND DISCUSSION

Syntheses of the Pyridine Complexes 11a,b and 14a,b. Our starting hypothesis was that the presence of two sterically demanding ligands (i.e., the thiolate and the NHC) in the 14-electron active catalyst is the main reason for the low activity of monothiolate-substituted catalysts, an idea that is consistent with the fact that the presence of an electron-withdrawing group at the benzylidene ether ligand only affects the catalytic activity marginally.[49] However, attempts to improve the activity by using smaller ligands resulted in less stable and less *Z*-selective catalysts.[48,49] Instead, we noted that DFT studies suggest that the low catalytic activity of thiolate-substituted catalyst **5** mainly is due to its slow initiation.[30,48] In particular, the calculations show that the dissociation of the chelating ether functionality should be fast, while the bottleneck of the reaction is the first metathesis step, which replaces the starting benzylidene ether ligand. The high energy of the transition state of this step is due to the steric repulsion between the bulky thiolate and the *o*-isopropoxybenzylidene.[30] Spurred by this insight, we inspected the transition state and found that the *o*-isopropoxy moiety was the most important contributor to the repulsion. This suggests that replacing the chelating 2-isopropoxybenzylidene ligand by a unsubstituted benzylidene and a suitable monodentate donor might lead to a more active precatalyst.

We set out to investigate monodentate neutral donors such as alkylphosphines, alkyl phosphites, and several N-heterocyclic compounds, and after a preliminary screening of donor-stabilized parent ruthenium-based catalysts, we identified pyridine as a suitable ligand.

The pyridine-stabilized version of **5**, i.e. complex **11a**, was successfully prepared by a two-step substitution starting from Grubbs second-generation catalyst **9** (see Scheme 1). First, tricyclohexylphosphine was replaced by two pyridine molecules to give **10** using a previously reported literature procedure.[54] Next, the target compound **11a** was obtained, in low yield (29%), by reacting **10** with potassium 2,4,6-triphenylbenzenethiolate (**8a**), which was prepared according to literature procedures starting from the commercially available 2,4,6-triphenylbenzenethiol.[47] The low yield of the second step is a consequence of the difficult separation of **11a** from unidentified alkylidene-free ruthenium species, some of which are presumably products of decomposition of **11a** (see the Supporting Information for details).

In order to evaluate the effect of a larger and more donating thiolate ligand in the framework of the new catalyst design, we prepared **11b**, which is based on a computationally designed thiolate ligand, 2,4,6-tris(3,5-dimethylphenyl)benzenethiolate (**8b**).[55] Reaction of **10** with **8b** delivered **11b** in fair yield

DOI: 10.1021/acs.organomet.7b00441
Organometallics 2017, 36, 3284−3292

Scheme 1. Synthesis of Complexes 11a,b[a]

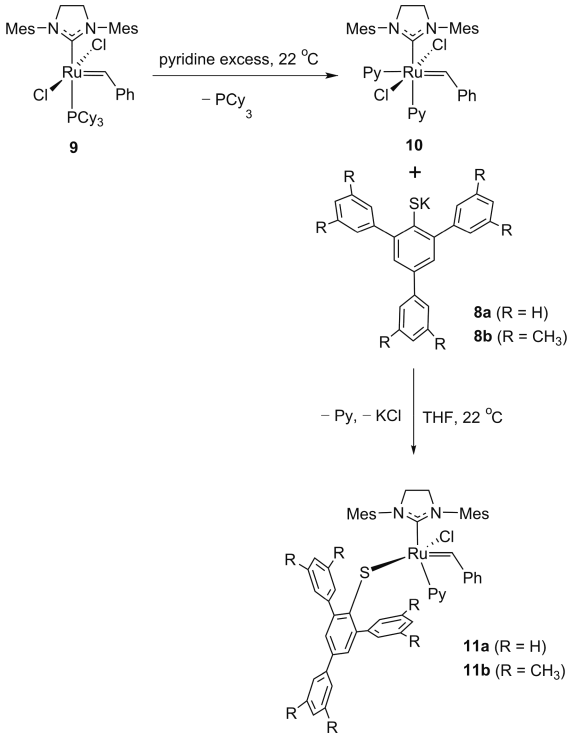

[a]Pyridine was the only neutral donor ligand for which Ru monothiolate alkylidene complexes could be isolated and purified. An analogue of **11b** based on 3-Br-pyridine was successfully isolated,[50] but this compound was harder to crystallize than **11b**, and we were unable to achieve a comparable level of purity for this 3-Br-pyridine analogue.

(60%). Crystals of **11b** suitable for X-ray diffraction analysis were grown at −34 °C from a solution of the complex, obtained by first dissolving **11b** in a minimum amount of toluene, followed by addition of pentane until the solution became slightly cloudy.

The molecular structure of **11b** and the relevant bond lengths and angles are shown in Figure 2. The complex has a slightly distorted square pyramidal geometry, with the benzylidene ligand occupying the apical position, oriented toward the less sterically demanding chloride ligand to avoid the bulky thiolate. A similar steric influence from the thiolate is evident also on the pyridine ligand. The S1−Ru1−N1 bond angle (92.3°) is wider than the corresponding angle involving chlorine (Cl1−Ru1−N1 = 84.1°), showing that the pyridine is bent toward the chloride to avoid the bulky thiolate. In contrast, even with the thiolate in a cis position, the ruthenium−pyridine bond distance is relatively short (2.132 Å) in comparison with, for example, those of similar pyridine-stabilized ruthenium alkylidenes (2.128−2.205 Å).[56] On the other hand, the other ruthenium—ligand bonds are slightly elongated, by 0.3 pm (alkylidene), 5 pm (NHC), 1 pm (chloride), and 3 pm (thiolate), respectively, in comparison with the corresponding bonds in **5**. The largest difference is observed for the NHC ligand, in agreement with the expected larger trans influence of the pyridine in comparison with the ether ligand. Finally, the bond angle at the sulfur atom (Ru1−S1−C1 = 107.6°) is, remarkably, 5° sharper than that of **5**, despite the smaller thiolate ligand of the latter compound.

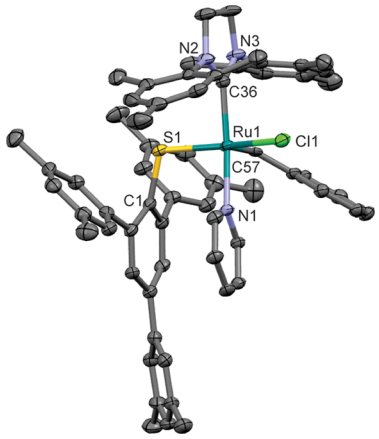

Figure 2. ORTEP-style drawing of one of the two unique complexes of **11b** with the anisotropic displacement ellipsoids drawn at the 30% probability level. Hydrogen atoms and solvent molecules (pentane) have been omitted for clarity. Selected geometrical parameters (bond distances in Å and angles in deg): Ru1−C57 = 1.831, Ru1−Cl1 = 2.404, Ru1−S1 = 2.340, Ru1−N1 = 2.132, Ru−C36 = 2.054; Ru1−S1−C1 = 107.6, S1−Ru1−Cl1 = 160.93, C36−Ru1−N1 = 167.3.

In order to probe the generality of our approach and the influence of ligand variation, we decided to repeat the same two-step protocol on the basis of another commercially available catalyst, CatMetium RF3[57] (**12**, Scheme 2). The

Scheme 2. Synthesis of Complexes 14a,b

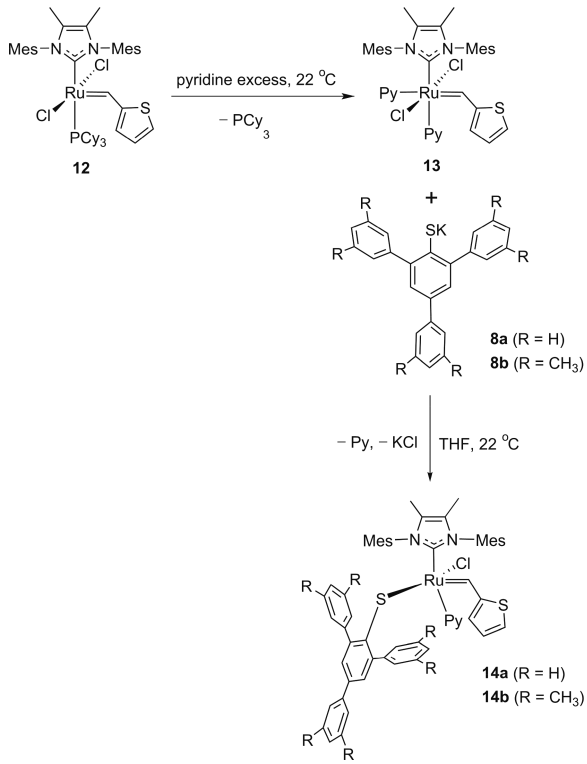

alkylidene ligand (2-thienylmethylidene) of complex **12** differs slightly from that of **8**, and **12** also contains an unsaturated NHC with a dimethyl-substituted backbone (Me_2IMes). Starting from **12**, we synthesized the new monothiolate-substituted catalysts **14a,b** as shown in Scheme 2. The bis-pyridine intermediate **13** was prepared in very good yield

DOI: 10.1021/acs.organomet.7b00441
Organometallics 2017, 36, 3284−3292

(84%) by reacting **12** with an excess of pyridine (see the Supporting Information for details). Next, the reaction of **13** with **8a** or **8b** delivered the target compound **14a** or **14b** in low (37%) and very good (82%) yields, respectively. As for **11a** above, which is also based on the 2,4,6-triphenylbenzenethiolate ligand, the low yield of **14a** resulted from its difficult isolation and purification. Crystals of **14b** were grown from a concentrated solution in pentane at −34 °C, and the X-ray diffraction analysis thereof revealed that the structure of **14b** (Figure 3) is similar to that of **11b** described above.

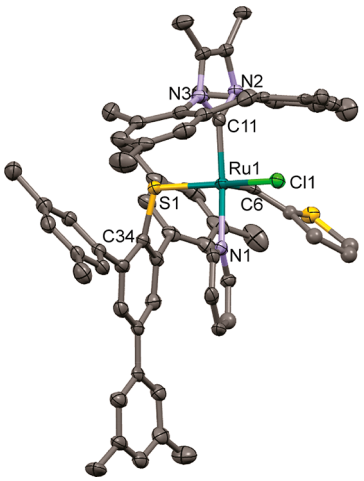

Figure 3. ORTEP-style drawing of one of the two unique complexes of **14b** with the anisotropic displacement ellipsoids drawn at the 50% probability level. Hydrogen atoms and solvent molecules (pentane) have been omitted for clarity. Selected geometrical parameters (bond distances in Å and angles in deg): Ru1−C6 = 1.832, Ru1−C11 = 2.066, Ru1−S1 = 2.335, Ru1−N1 = 2.141, Ru−Cl1 = 2.405; Ru1−S1−C34 = 108.7, S1−Ru1−Cl1 = 159.63, C11−Ru1−N1 = 168.1.

Dissociation Equilibrium of Pyridine Ligand in Solution. The ^{1}H NMR spectra (C_6D_6) of **11a,b** and **14a,b** reveal that these 16-electron complexes A easily dissociate the pyridine ligand in solution to give the corresponding 14-electron species B, as depicted in Scheme 3. Specifically, the ^{1}H

Scheme 3. Dissociation Equilibrium of the Pyridine Ligand in C_6D_6 Solution

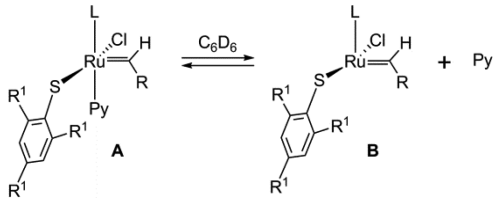

NMR spectra contain two different signals for the alkylidene proton along with the signals corresponding to the free pyridine ligand. The pyridine signals are equimolar with the alkylidene proton signal located at higher field strength (lower δ), which is due to the 14-electron complex B. This lability is unusual for a pyridine-stabilized 16-electron complex, because pyridine is flat and has a high affinity for the ruthenium center[58,59] and because the dissociation produces an electronically as well as coordinatively unsaturated ruthenium species B. These species, albeit observed only in solution, are rare examples of stable, neutral tetracoordinate NHC-based ruthenium alkylidenes. Whereas several cationic NHC-bearing, tetracoordinate ruthenium alkylidenes have been reported and characterized by X-ray diffraction,[41,60−62] the only known neutral counterparts are based on a trialkylphosphine in combination with two sterically demanding alkoxide ligands.[63,64]

The fraction of B formed depends on the nature of the pyridine-stabilized complex A and increases with temperature and dilution; see Table 1 and Table S1 in the Supporting

Table 1. Dissociation of Pyridine from 11a,b and 14a,b in C_6D_6 Solution (5 mM)

		amt of B (%)	
entry	complex	293 K	313 K
1	**11a**	3.8	8.2
2	**11b**	11.8	24.7
3	**14a**	4.1	7.0
4	**14b**	18.4	32.2

Information. In particular, more B is produced by the two complexes having the bulkier and more electron donating thiolate ligand, and at 313 K almost a fourth and a third of the **11b** and the **14b** complexes, respectively, have dissociated the pyridine ligand. In comparison, the influence of the two carbene ligands (i.e., the NHC and the alkylidene) is less clear. For example, at 293 K the percentage of B increases in the order **11a** < **14a** ≪ **11b** ≪ **14b**, while at 313 K **14a** becomes the complex least prone to dissociation, giving the order **14a** < **11a** ≪ **11b** < **14b** (see Table 1 and the Supporting Information for more details).

In order to understand these trends and the factors favoring pyridine dissociation, van't Hoff plots have been generated to determine the thermodynamic parameters ($\Delta H°$ and $\Delta S°$; see Figure 4 and Table 2). The dissociation constant (K) in C_6D_6

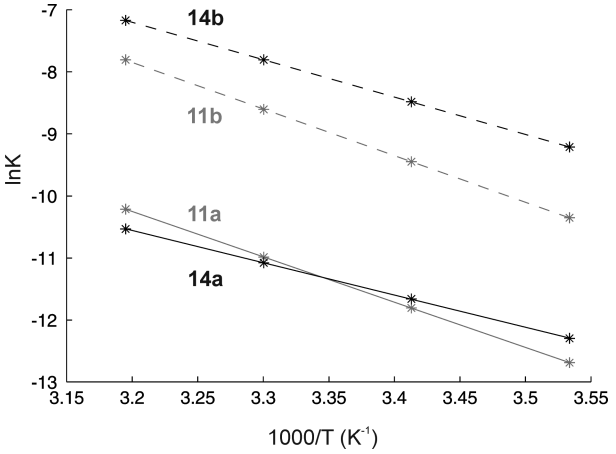

Figure 4. van't Hoff plots of ln K vs 1000/T for the dissociation equilibrium of pyridine in C_6D_6 solution (5 mM) of **11a,b** and **14a,b**.

Table 2. Experimentally Determined Thermodynamic Parameters for Pyridine Dissociation from 11a,b and 14a,b

entry	complex	ΔH (kcal/mol)	ΔS (cal/mol)
1	**11a**	14.51(6)	26.1(2)
2	**11b**	14.9(2)	32.1(5)
3	**14a**	10.3(2)	12.1(5)
4	**14b**	11.97(9)	24.0(3)

DOI: 10.1021/acs.organomet.7b00441
Organometallics 2017, 36, 3284−3292

solution (5 mM) has been evaluated at four different temperatures (283, 293, 303, and 313 K) for all four complexes using ^{1}H NMR spectroscopy (see the Supporting Information). In all cases the equilibrium was reached instantaneously, suggesting a negligible or very low dissociation barrier. Figure 4 shows the plot of ln K against 1000/T, while the calculated $\Delta H°$ and $\Delta S°$ values of dissociation, i.e., the slope and the intercept of the lines, respectively, are reported in Table 2. Both the enthalpy and the entropy of dissociation are positive for all four complexes. In terms of enthalpy, dissociation costs more than 10 kcal/mol in all cases, but the positive entropy changes (12−32 cal/mol) imply that the Gibbs free energies of dissociation are modest (4.5−6.5 kcal/mol) at 313 K, consistent with the substantial fractions of pyridine dissociated at that temperature (Table 1).

Even if the thermochemical parameters of Table 2 are all positive, the thiolate-substituted catalysts (**14**) based on parent complex **12** (CatMetium RF3) have lower enthalpies and entropies of dissociation in comparison to those based on **9** (the second-generation Grubbs catalyst). Dissociation is in particular associated with small thermochemical parameters for complex **14a** ($\Delta H°$ = 10.3(2) kcal/mol, $\Delta S°$ = 12.1(5) cal/mol), which might suggest that dissociation of pyridine partially is compensated for by dimerization of B (i.e., **14a** without pyridine). Reversible formation of dimers of 14-electron complexes has been demonstrated by Piers and co-workers for their tetracoordinate ruthenium phosphonium alkylidenes,[65] and the tendency to form aggregates grows with increasing complex concentration.[65] Indeed, doubling the concentration of the complex lowers the enthalpy and entropy of dissociation ($\Delta H°$ = 7.0(2) kcal/mol, $\Delta S°$ = 1.6(4) cal/mol, at [**14a**] = 10 mM; see the Supporting Information for details). However, even if these data suggest that the dissociated species B of **14a** do form aggregates, the ^{1}H NMR spectra of **14a** recorded at the two different concentrations do not provide evidence for aggregate formation. The corresponding spectra, recorded at 283 K and at 5 and 10 mM, respectively, may essentially be superimposed and the signals associated with aggregates cannot be distinguished from the rest of the signals. These spectra are complex, and the aggregate-related signals are presumably masked by other signals (see the Supporting Information for details).

In the absence of spectral evidence for aggregation, the contrast between the low dissociation entropy of **14a** and those of **11b** ($\Delta S°$ = 32.1(5) cal/mol), **11a** ($\Delta S°$ = 26.1(2) cal/mol), and **14b** ($\Delta S°$ = 24.0(3) cal/mol) is perhaps the most telling piece of information. The much higher dissociation entropies of **11a,b** and **14b** suggest that their the tendency to form aggregates of B must be low, which is consistent with the fact that $\Delta H°$ and $\Delta S°$ of these complexes decrease much less than those of **14a** when the concentration of the complex is doubled (see Table S1 in the Supporting Information).

Catalytic Performance in Olefin Metathesis. Complexes **11a,b** and **14a,b** were initially tested in the self-metathesis of neat allylbenzene, a highly reactive substrate that is also prone to double-bond alkene migration in the presence of ruthenium-based olefin metathesis catalysts,[26,66−68] at room temperature using a catalyst loading of 1 mol % (see Table 3). As a background for the evaluation of the new catalysts, the original monothiolate-substituted catalysts **5** and **6** (containing a chelating *o*-isopropoxybenzylidene ligand) were also tested under identical conditions. The reaction was quenched after 5 min by dilution of the mixture with hexane followed by filtration through a short pad of silica gel to remove the catalyst.[69]

Table 3. Self-Metathesis of Neat Allylbenzene at 22 °C

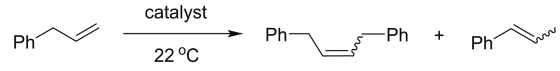

15 **16** **17**

entry	cat.	**16**/**17**[a]	yield of **16** (%)[b]	*Z*-**16** (%)[a]
1	**5**	0.2	2	83
2	**6**	0.6	3	87
3	**11a**	15	41	81
4	**11b**	51	33	86
5	**14a**	63	69	63
6	**14b**	>100	73	80

[a]Determined by ^{1}H NMR analysis of the quenched reaction mixture. [b]Isolated yields.

The pyridine-stabilized complexes **11a,b** and **14a,b** gave isolated yields in the range 33−73%, which is clearly superior to the single-digit yields of **5** and **6** (Table 3). In addition to being more active, the pyridine-stabilized precatalysts are also much more selective for metathesis, with a lower tendency to isomerize the substrate, as shown by their higher ratios **16**/**17**.

The catalytic performances of precursors such as **11a** and **5** differ radically, even though they should give the same active species on initiation. This strongly suggests that the faster initiation of the pyridine-stabilized precatalysts is the cause of their much lower tendency to isomerization. Olefin isomerization during metathesis is believed to be promoted not by the olefin metathesis catalyst but by different ruthenium-based catalyst decomposition products or impurities present in the precatalyst.[47] Thus, rapid initiation of the metathesis catalyst ensures that, for a certain time interval at the beginning of the reaction, the ratio of metathesis-active to isomerization-active ruthenium species will be high.

Since the species promoting isomerization of the substrate also contribute to erosion of the stereoselectivity,[47] increasing the initiation rate of the catalyst may represent a strategy to improve the efficiency of many stereoselective transformations. Grubbs and co-workers have recently reported that faster-initiating catalysts perform far better in *E*-stereoretentive cross-metathesis than their slower-initiating counterparts.[28] In contrast, Nelson and Percy, studying a range of catalysts based on leaving phosphine ligands as well as chelating alkylidenes, reported that the tendency to isomerization did not correlate with the initiation rate but was instead heavily affected by the nature of the dissociating ligand.[70] Their findings may offer an alternative, or additional, explanation for the superiority of **11a** in comparison to **5**.

In addition to shedding light on the role of the initiation rate, the catalytic results in Table 3 show that yields and selectivities also depend on the nature of the remaining ligands. For example, the complexes **11a,b** derived from the Grubbs second-generation catalyst are less active and more prone to substrate isomerization than **14a,b** prepared from CatMetium RF3, but the latter are less *Z*-selective (cf. entries 3 and 5 and entries 4 and 6 in Table 3). Similarly, the nature of the thiolate ligand mainly affects the tendency to isomerization and the *Z* selectivity, and in particular the complexes based on 2,4,6-tris(3,5-dimethylphenyl)benzenethiolate are more selective for metathesis as well as for the *Z* product in comparison to those based on the smaller 2,4,6-triphenylbenzenethiolate. In

DOI: 10.1021/acs.organomet.7b00441
Organometallics 2017, 36, 3284−3292

conclusion, the selectivity decreases in the order **11b** > **11a** and **14b** > **14a**. Overall, **14b** stands out as the most active and efficient catalyst.

Next, the catalytic performance of **14b** was tested in the self-metathesis of six additional substrates, as depicted in Figure 5.

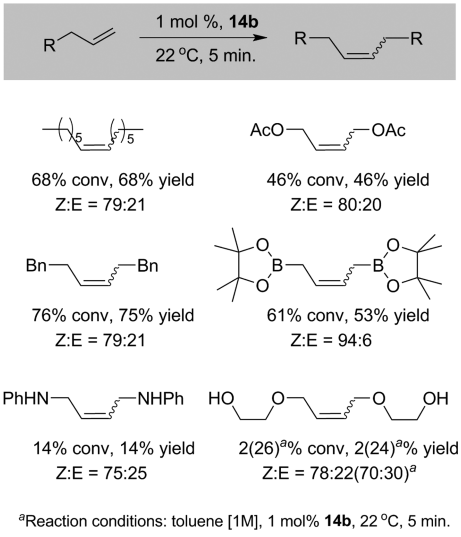

Figure 5. Self-metathesis of neat 1-alkenes with catalyst **14b**.

The reactions were conducted under conditions identical with those above for allylbenzene, except for the presence of hexamethylbenzene as internal standard. After 5 min the reaction was quenched with an excess of ethyl vinyl ether (EVE) and then a sample of the reaction mixture was analyzed by ^{1}H NMR spectroscopy.

Of the six olefinic substrates tested, two, *N*-allylaniline and 2-allyloxyethanol, gave low yields (14% and 2%, respectively) and less than 80% of the *Z* product. For 2-allyloxyethanol, the low solubility of **14b** in this substrate, as indicated by the heterogeneous appearance of the reaction mixture, to a large extent explains the near-absence of product. Indeed, when the same reaction was performed in toluene (1 M), under otherwise identical conditions, a much higher yield (24%) was obtained, albeit with a smaller fraction of the *Z* product (70%).

The four remaining substrates (1-octene, allylacetate, 4-phenyl-1-butene, and allylboronic acid pinacol ester) were all converted to self-metathesis products in fair to good yields (46−75%) in combination with moderate to high *Z* selectivities (79−94%). Remarkably, these results were obtained in only 5 min and at room temperature and, with the exception of one substrate (allylboronic acid pinacol ester), the degree of isomerization, given by the difference between conversion and yield, is negligible or very low.

Inspired by these results, the self-metathesis of substrates (*ω*-alkenoic acids) bearing acidic functional groups that have proved challenging for other *Z*-selective catalysts[52,71] was also tested (see Table 4). The cis products of this self-metathesis are valuable and may, for example, be used as key intermediates in the synthesis of several pharmaceutical drugs[72−77] and natural products.[78,79] The latter compounds, which are traditionally prepared via multistep procedures often developed for specific target molecules,[79,80] can be reached more directly via *Z*-selective self-metathesis of *ω*-alkenoic acids.

Table 4. Self-Metathesis of *ω*-Alkenoic Acids in Toluene Solution (1 M)

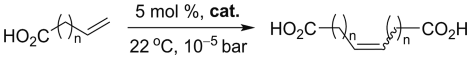

entry	cat.	*n*	time (min)	conversn (%)[a]	yield (%)[a]	*Z* (%)[a]
1	**9**	2	5	6	6	15
			25	24	24	12
			60	46	45	8
2	**14b**	2	5	35	35	80
			25	44	42	70
			60	50	42	54
3	**6**	8	5	10	3	n.d.
4	**11b**	8	5	34	28	45
5	**14b**	8	5	59	56	67

[a]Determined by ^{1}H NMR analysis of quenched reaction mixture samples using hexamethylbenzene as internal standard. Samples of the reaction mixture were taken at regular intervals and immediately quenched using an excess of ethyl vinyl ether (EVE). Conversion is the amount of substrate converted, whereas yield refers to the amount of substrate converted into the self-metathesis product.

The reaction was conducted at room temperature in toluene (1 M), under static vacuum (10^{-5} bar) and using 5 mol % of catalyst.

Entry 2 of Table 4 shows that the self-metathesis of 4-pentenoic acid using **14b** is fast and clean during the first few minutes, but the activity drops rapidly with the progress of the reaction, probably as a consequence of catalyst decomposition, as indicated by the onset of double-bond migration and diverging values for conversions and yields. For example, after 5 min 35% of the self-metathesis product was obtained with 80% *Z* selectivity, while another 20 min only resulted in a modestly improved yield, some product impurity (ca. 2%) due to double-bond migration in the substrate, and a drop in *Z* selectivity. Beyond 25 min of reaction time, no more self-metathesis product is formed. More isomerization products are formed, however, and the erosion of the *Z* selectivity continues. Such erosion is, in fact, also seen for Grubbs second-generation catalyst **9** (entry 1 in Table 4), which was subjected to the same test as **14b**. In contrast to the case for **14b**, however, the reaction using **9** is slow at the beginning but the rate increases with the progress of the reaction, with the *E* isomer being the major product.

Another series of self-metathesis experiments, under conditions identical with those of the 4-pentenoic acid conversions above, was carried out using a longer substrate, 10-undecenoic acid. Using catalyst **14b** (entry 5), the reaction was faster than for 4-pentenoic acid, and after 5 min more than 60% of the substrate had been converted, mostly to the self-metathesis product (57%), with moderate *Z*-selectivity (67%). Complex **11b** also promotes this reaction, but with both lower activity and *Z* selectivity in comparison to **14b**. In contrast, **6**, which contains a chelating alkylidene ligand and which tolerates acidic additives,[47] is a poor metathesis catalyst for this substrate and mainly promotes double-bond migration in the substrate (entry 3).

Finally, catalyst **14b** was also tested in macrocyclic ring-closing metathesis (mRCM) of two different dienes, **18** and **19**, whose products are **18a**, the *Z* isomer of which is the Yuzu lactone,[81,82] a 13-membered lactone used in the fragrance industry, and the 14-membered lactone **19a**, respectively (Scheme 4). These lactones have previously been prepared

DOI: 10.1021/acs.organomet.7b00441
Organometallics 2017, 36, 3284−3292

Scheme 4. Macrocylic Ring-Closing Metathesis Using 14b

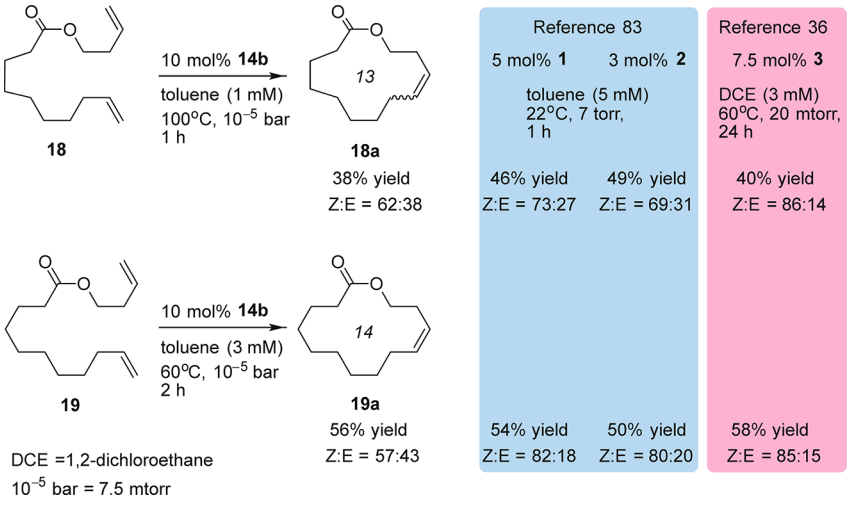

via *Z*-selective mRCM using both the cyclometalated ruthenium-based catalyst **3**[36] and the monoaryloxide−pyrrolide (MAP) tungsten- and molybdenum-based catalysts **1** and **2**[83] (see Scheme 4 and Chart 1 for the catalyst structures). The results from these tests can be used in the evaluation of **14b**. The mRCM reactions of **14b** were carried out under partially optimized conditions,[50] including the use of static vacuum (10^{-5} bar), high substrate dilution (in toluene), elevated temperature, and high catalyst loading (10%).

Macrocyclization of **18** is more challenging than that of **19**, because the product is a 13-membered lactone and is more strained than the 14-membered **19a**.[83] The reactions were thus conducted under slightly different conditions, with a reaction temperature of 60 °C, a substrate concentration of 3 mM, and quenching after 2 h being used for **19**, whereas a higher temperature (100 °C), a higher substrate dilution (1 mM), and quenching after 1 h were used for the more difficult reaction of diene **18**.

The products of mRCM of **18** and **19** were purified using silica gel chromatography, and the *Z* content was determined by ^{1}H NMR spectroscopy following literature procedures.[36] Lactones **18a** and **19a** were isolated in 38% and 56% yields, respectively, with *Z* selectivities of 62% and 57%. Although both the MAP catalysts (**1** and **2**) and the cyclometalated ruthenium catalysts (**3**) have given higher *Z* selectivities, the yields are comparable (see Scheme 4). The yields and reaction times of **14b** are particularly impressive in comparison with the earlier generations of bottom-pathway monothiolate-substituted catalysts, which hardly promoted mRCM reactions at all,[50] demonstratring that even small changes in molecular structure of a precatalyst may have dramatic consequences for the catalytic performance. Specifically, as we have seen, the low apparent activity of the *o*-isopropoxybenzylidene-coordinated catalysts is due to slow initiation, and replacing the alkylidene ether chelate with a nonchelating carbene and a pyridine drastically improves the catalytic efficiency.

CONCLUSIONS

A new class of highly active and *Z*-selective Ru monothiolate alkylidenes for olefin metathesis has been developed. These 16-electron compounds are stabilized by a pyridine molecule and are prepared in one step by reacting readily accessible pyridine-stabilized third-generation Grubbs-type catalysts with the corresponding potassium thiolate. Remarkably, the pyridine molecule easily dissociates in solution, releasing a substantial fraction of the 14-electron metathesis-active species even at low temperature and at relatively high catalyst concentrations. The facile pyridine dissociation and a sterically nondemanding monodentate alkylidene ligand ensure that these precatalysts initiate quickly. In comparison to the previously reported catalysts based on the *o*-isopropoxybenzylidene chelate, the new fast-initiating catalysts are much more selective toward olefin metathesis, due to their reduced tendency to olefin isomerization, while maintaining a comparable *Z* selectivity. They reach a moderate to high *Z* selectivity with appreciable yields in self-metathesis of terminal olefins after only a few minutes at room temperature for most of the tested substrates. They tolerate acidic substrates and mediate the first[52,53] *Z*-selective synthesis of α,ω-dicarboxylic acid alkenes via self-metathesis of ω-alkenoic acids. Finally, they are also efficient at the high substrate dilutions of macrocylic ring closing metathesis and resist temperatures up to and above 100 °C.

ASSOCIATED CONTENT

Supporting Information

The Supporting Information is available free of charge on the ACS Publications website at DOI: 10.1021/acs.organomet.7b00441.

Experimental details, additional spectral and analytical data, and crystallographic data for **11b** and **14b** (PDF)

Accession Codes

CCDC 1543473−1543474 contain the supplementary crystallographic data for this paper. These data can be obtained free of charge via www.ccdc.cam.ac.uk/data_request/cif, or by emailing data_request@ccdc.cam.ac.uk, or by contacting The Cambridge Crystallographic Data Centre, 12 Union Road, Cambridge CB2 1EZ, UK; fax: +44 1223 336033.

AUTHOR INFORMATION

Corresponding Authors

*E-mail for G.O.: Giovanni.Occhipinti@uib.no.
*E-mail for V.R.J.: Vidar.Jensen@uib.no.

ORCID

Giovanni Occhipinti: 0000-0002-7279-6322
Karl W. Törnroos: 0000-0001-6140-5915

DOI: 10.1021/acs.organomet.7b00441
Organometallics 2017, 36, 3284−3292

Vidar R. Jensen: 0000-0003-2444-3220

Notes

The authors declare no competing financial interest.

■ ACKNOWLEDGMENTS

The authors gratefully acknowledge financial support from the Research Council of Norway via the GASSMAKS (grant number 208335) and FORNY2020 (239288) programs and via the Norwegian NMR Platform, NNP (226244). The authors also thank Nataliya Kostenko for a preliminary screening of monodentate donors and parent ruthenium-based catalysts from which to start the synthesis of complexes **11** and **14** and Theresa Schilling for preparing lactone **18a**. Bjarte Holmelid is thanked for assistance with the HRMS (DART and ESI$^-$) analyses.

■ REFERENCES

(1) Hoveyda, A. H.; Zhugralin, A. R. *Nature* **2007**, *450*, 243−251.
(2) *Handbook of metathesis*, 2nd ed.; Grubbs, R. H., Wenzel, A. G., O'Leary, D. J., Khosravi, E., Eds.; Wiley-VCH: Weinheim, Germany, 2015; Vols. *1*−*3*.
(3) Higman, C. S.; Lummiss, J. A. M.; Fogg, D. E. *Angew. Chem., Int. Ed.* **2016**, *55*, 3552−3565.
(4) Mol, J. C. *J. Mol. Catal. A: Chem.* **2004**, *213*, 39−45.
(5) Trnka, T. M.; Grubbs, R. H. *Acc. Chem. Res.* **2001**, *34*, 18−29.
(6) Clavier, H.; Grela, K.; Kirschning, A.; Mauduit, M.; Nolan, S. P. *Angew. Chem., Int. Ed.* **2007**, *46*, 6786−6801.
(7) Samojlowicz, C.; Borre, E.; Mauduit, M.; Grela, K. *Adv. Synth. Catal.* **2011**, *353*, 1993−2002.
(8) Borre, E.; Rouen, M.; Laurent, I.; Magrez, M.; Caijo, F.; Crevisy, C.; Solodenko, W.; Toupet, L.; Frankfurter, R.; Vogt, C.; Kirschning, A.; Mauduit, M. *Chem. - Eur. J.* **2012**, *18*, 16369−16382.
(9) Gleeson, E. C.; Jackson, W. R.; Robinson, A. J. *Tetrahedron Lett.* **2016**, *57*, 4325−4333.
(10) Chhabra, S.; Belgi, A.; Bartels, P.; van Lierop, B. J.; Robinson, S. D.; Kompella, S. N.; Hung, A.; Callaghan, B. P.; Adams, D. J.; Robinson, A. J.; Norton, R. S. *J. Med. Chem.* **2014**, *57*, 9933−9944.
(11) Guidone, S.; Songis, O.; Nahra, F.; Cazin, C. S. J. *ACS Catal.* **2015**, *5*, 2697−2701.
(12) Binder, J. B.; Raines, R. T. *Curr. Opin. Chem. Biol.* **2008**, *12*, 767−773.
(13) Sundararaju, B.; Sridhar, T.; Achard, M.; Sharma, G. V. M; Bruneau, C. *Eur. J. Org. Chem.* **2013**, *2013*, 6433−6442.
(14) Bidange, J.; Fischmeister, C.; Bruneau, C. *Chem. - Eur. J.* **2016**, *22*, 12226−12244.
(15) Samojlowicz, C.; Bieniek, M.; Zarecki, A.; Kadyrov, R.; Grela, K. *Chem. Commun.* **2008**, 6282−6284.
(16) Weitekamp, R. A.; Atwater, H. A.; Grubbs, R. H. *J. Am. Chem. Soc.* **2013**, *135*, 16817−16820.
(17) Astruc, D.; Diallo, A. K.; Gatard, S.; Liang, L. Y.; Ornelas, C.; Martinez, V.; Mery, D.; Ruiz, J. *Beilstein J. Org. Chem.* **2011**, *7*, 94−103.
(18) Liu, X.; Basu, A. *J. Organomet. Chem.* **2006**, *691*, 5148−5154.
(19) Salinas, B.; Ruiz-Cabello, J.; Lechuga-Vieco, A. V.; Benito, M.; Herranz, F. *Chem. - Eur. J.* **2015**, *21*, 10450−10456.
(20) Bertrand, A.; Hillmyer, M. A. *J. Am. Chem. Soc.* **2013**, *135*, 10918−10921.
(21) Torker, S.; Koh, M. J.; Khan, R. K. M.; Hoveyda, A. H. *Organometallics* **2016**, *35*, 543−562.
(22) Flook, M. M.; Jiang, A. J.; Schrock, R. R.; Müller, P.; Hoveyda, A. H. *J. Am. Chem. Soc.* **2009**, *131*, 7962−7963.
(23) Jiang, A. J.; Zhao, Y.; Schrock, R. R.; Hoveyda, A. H. *J. Am. Chem. Soc.* **2009**, *131*, 16630−16631.
(24) Endo, K.; Grubbs, R. H. *J. Am. Chem. Soc.* **2011**, *133*, 8525−8527.
(25) Khan, R. K. M.; Torker, S.; Hoveyda, A. H. *J. Am. Chem. Soc.* **2013**, *135*, 10258−10261.
(26) Occhipinti, G.; Hansen, F. R.; Törnroos, K. W.; Jensen, V. R. *J. Am. Chem. Soc.* **2013**, *135*, 3331−3334.
(27) Johns, A. M.; Ahmed, T. S.; Jackson, B. W.; Grubbs, R. H.; Pederson, R. L. *Org. Lett.* **2016**, *18*, 772−775.
(28) Ahmed, T. S.; Grubbs, R. H. *J. Am. Chem. Soc.* **2017**, *139*, 1532−1537.
(29) Liu, P.; Xu, X.; Dong, X.; Keitz, B. K.; Herbert, M. B.; Grubbs, R. H.; Houk, K. N. *J. Am. Chem. Soc.* **2012**, *134*, 1464−1467.
(30) Nelson, J. W.; Grundy, L. M.; Dang, Y.; Wang, Z.-X.; Wang, X. *Organometallics* **2014**, *33*, 4290−4294.
(31) Koh, M. J.; Nguyen, T. T.; Lam, J. K.; Torker, S.; Hyvl, J.; Schrock, R. R.; Hoveyda, A. H. *Nature* **2017**, *542*, 80−85.
(32) Fürstner, A. *Science* **2013**, *341*, 1357−1364.
(33) Shahane, S.; Bruneau, C.; Fischmeister, C. *ChemCatChem* **2013**, *5*, 3436−3459.
(34) Herbert, M. B.; Grubbs, R. H. *Angew. Chem., Int. Ed.* **2015**, *54*, 5018−5024.
(35) Werrel, S.; Walker, J. C. L.; Donohoe, T. J. *Tetrahedron Lett.* **2015**, *56*, 5261−5268.
(36) Marx, V. M.; Herbert, M. B.; Keitz, B. K.; Grubbs, R. H. *J. Am. Chem. Soc.* **2013**, *135*, 94−97.
(37) Marx, V. M.; Rosebrugh, L. E.; Herbert, M. B.; Grubbs, R. H. *Top. Organomet. Chem.* **2014**, *48*, 1−17.
(38) Koh, M. J.; Khan, R. K. M.; Torker, S.; Yu, M.; Mikus, M. S.; Hoveyda, A. H. *Nature* **2015**, *517*, 181−186.
(39) Vyboishchikov, S. E.; Bühl, M.; Thiel, W. *Chem. - Eur. J.* **2002**, *8*, 3962−3975.
(40) Romero, P. E.; Piers, W. E. *J. Am. Chem. Soc.* **2005**, *127*, 5032−5033.
(41) Wenzel, A. G.; Grubbs, R. H. *J. Am. Chem. Soc.* **2006**, *128*, 16048−16049.
(42) Benitez, D.; Tkatchouk, E.; Goddard, W. A., III *Chem. Commun.* **2008**, 6194−6196.
(43) Conrad, J. C.; Parnas, H. H.; Snelgrove, J. L.; Fogg, D. E. *J. Am. Chem. Soc.* **2005**, *127*, 11882−11883.
(44) Torker, S.; Müller, A.; Sigrist, R.; Chen, P. *Organometallics* **2010**, *29*, 2735−2751.
(45) Teo, P.; Grubbs, R. H. *Organometallics* **2010**, *29*, 6045−6050.
(46) Jensen, V. R.; Occhipinti, G.; Hansen, F. U.S. Patent 8,716,488 B2, 2014.
(47) Occhipinti, G.; Koudriavtsev, V.; Törnroos, K. W.; Jensen, V. R. *Dalton Trans.* **2014**, *43*, 11106−11117.
(48) Smit, W.; Koudriavtsev, V.; Occhipinti, G.; Törnroos, K. W.; Jensen, V. R. *Organometallics* **2016**, *35*, 1825−1837.
(49) Jensen, V. R.; Occhipinti, G. *Novel Organometallic Catalysts*. U.S. Patent US 9,303,100 B2, Apr 5, 2016.
(50) Jensen, V. R.; Occhipinti, G. *Improved olefin metathesis catalysts*. Int. Patent Appl. WO 2017009232, 2017.
(51) Bates, J. M. Ruthenium Catalysts for Olefin Metathesis: Understanding the Boomerang Mechanism and Challenges Associated with Stereoselectivity. Ph.D. thesis, University of Ottawa, Ottawa, ON, Canada K1N 6N5, 2014.
(52) Keitz, B. K.; Endo, K.; Herbert, M. B.; Grubbs, R. H. *J. Am. Chem. Soc.* **2011**, *133*, 9686−9688.
(53) Highly stereoretentive cross-metathesis between (*Z*)-2-butene-1,4-diol and carboxylic acid containing substrates has been reported with ruthenium catecholthiolate catalysts.[38] However, *Z*-selective self-metathesis of 1-alkenecarboxylic acid containing substrates has not yet been reported.
(54) Sanford, M. S.; Love, J. A.; Grubbs, R. H. *J. Am. Chem. Soc.* **2001**, *123*, 6543−6554.
(55) Occhipinti, G.; Vitali, K.; Tönroos, K. W.; Jensen, V. R. To be submitted for publication.
(56) The Cambridge Structural Database (CSD) of Cambridge Crystallographic Data Centre (CCDC), version 5.37, updated May 2016.
(57) Kadyrov, R.; Wolf, D.; Azap, C.; Ostgard, D. J. *Top. Catal.* **2010**, *53*, 1066−1072.

DOI: 10.1021/acs.organomet.7b00441
Organometallics 2017, 36, 3284−3292

(58) Poater, A.; Cavallo, L. *Beilstein J. Org. Chem.* **2015**, *11*, 1767−1780.
(59) Trzaskowski, B.; Grela, K. *Organometallics* **2013**, *32*, 3625−3630.
(60) Romero, P. E.; Piers, W. E.; McDonald, R. *Angew. Chem., Int. Ed.* **2004**, *43*, 6161−6165.
(61) Dubberley, S. R.; Romero, P. E.; Piers, W. E.; McDonald, R.; Parvez, M. *Inorg. Chim. Acta* **2006**, *359*, 2658−2664.
(62) Songis, O.; Slawin, A. M. Z.; Cazin, C. S. J. *Chem. Commun.* **2012**, *48*, 1266−1268.
(63) Sanford, M. S.; Henling, L. M.; Day, M. W.; Grubbs, R. H. *Angew. Chem., Int. Ed.* **2000**, *39*, 3451−3453.
(64) Coalter, J. N.; Bollinger, J. C.; Eisenstein, O.; Caulton, K. G. *New J. Chem.* **2000**, *24*, 925−927.
(65) Leitao, E. M.; van der Eide, E. F.; Romero, P. E.; Piers, W. E.; McDonald, R. *J. Am. Chem. Soc.* **2010**, *132*, 2784−2794.
(66) Keitz, B. K.; Endo, K.; Patel, P. R.; Herbert, M. B.; Grubbs, R. H. *J. Am. Chem. Soc.* **2012**, *134*, 693−699.
(67) Hassam, M.; Taher, A.; Arnott, G. E.; Green, I. R.; van Otterlo, W. A. L. *Chem. Rev.* **2015**, *115*, 5462−5569.
(68) Higman, C. S.; Plais, L.; Fogg, D. E. *ChemCatChem* **2013**, *5*, 3548−3551.
(69) This particular quenching procedure was used here because it facilitates the separation of the organic compounds from the least polar Ru catalysts (**14a**,**b** and **11b**) via silica gel filtration. Using EVE as a quenching reagent instead results in a partial elution (leaching) of colored ruthenium species.
(70) Nelson, D. J.; Percy, J. M. *Dalton Trans.* **2014**, *43*, 4674−4679.
(71) Keitz, B. K. In *Handbook of metathesis*, 2nd ed.; Grubbs, R. H., Wenzel, A. G., O'Leary, D. J., Khosravi, E., Eds.; Wiley-VCH: Weinheim, Germany, 2015; Vol. 3.
(72) Burlison, J. A.; Blagg, B. S. J. *Org. Lett.* **2006**, *8*, 4855−4858.
(73) Kusuma, B. R.; Peterson, L. B.; Zhao, H.; Vielhauer, G.; Holzbeierlein, J.; Blagg, B. S. J. *J. Med. Chem.* **2011**, *54*, 6234−6253.
(74) Perlman, N.; Albeck, A. *Synth. Commun.* **2000**, *30*, 4443−4449.
(75) Gensler, W. J.; Prasad, R. S.; Chaudhuri, A. P.; Alam, I. *J. Org. Chem.* **1979**, *44*, 3643−3652.
(76) Jayasuriya, N.; Bosak, S.; Regen, S. L. *J. Am. Chem. Soc.* **1990**, *112*, 5844−5850.
(77) Jayasuriya, N.; Bosak, S.; Regen, S. L. *J. Am. Chem. Soc.* **1990**, *112*, 5851−5854.
(78) Hagiwara, H.; Adachi, T.; Nakamura, T.; Hoshi, T.; Suzuki, T. *Nat. Prod. Commun.* **2012**, *7*, 913−915.
(79) Gensler, W. J.; Schlein, H. N. *J. Am. Chem. Soc.* **1955**, *77*, 4846−4849.
(80) Matson, J. B.; Grubbs, R. H. *Macromolecules* **2010**, *43*, 213−221.
(81) Rodefeld, L.; Tochtermann, W. *Tetrahedron* **1998**, *54*, 5893−5898.
(82) Fürstner, A.; Guth, O.; Rumbo, A.; Seidel, G. *J. Am. Chem. Soc.* **1999**, *121*, 11108−11113.
(83) Wang, C.; Yu, M.; Kyle, A. F.; Jakubec, P.; Dixon, D. J.; Schrock, R. R.; Hoveyda, A. H. *Chem. - Eur. J.* **2013**, *19*, 2726−2740.

DOI: 10.1021/acs.organomet.7b00441
Organometallics 2017, 36, 3284−3292